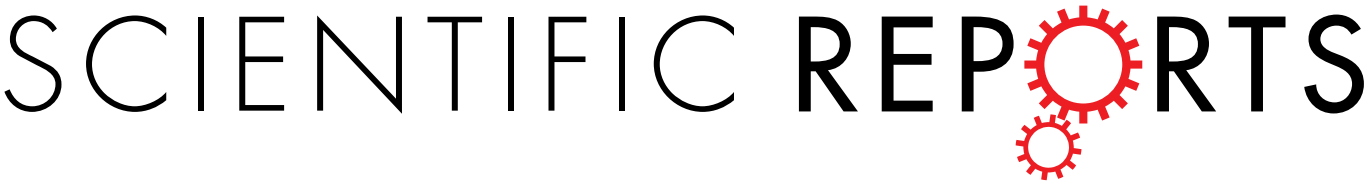

OPEN

The rate of quasiparticle recombination probes the onset of coherence in cuprate superconductors

Received: 11 February 2016
Accepted: 03 March 2016
Published: 13 April 2016

J. P. Hinton[1,2,3], E. Thewalt[1,2], Z. Alpichshev[4], F. Mahmood[4], J. D. Koralek[1,9], M. K. Chan[5], M. J. Veit[5], C. J. Dorow[5], N. Barišić[5,6], A. F. Kemper[1,10], D. A. Bonn[7,8], W. N. Hardy[7,8], Ruixing Liang[7,8], N. Gedik[4], M. Greven[5], A. Lanzara[1,2] & J. Orenstein[1,2]

In the underdoped copper-oxides, high-temperature superconductivity condenses from a nonconventional metallic "pseudogap" phase that exhibits a variety of non-Fermi liquid properties. Recently, it has become clear that a charge density wave (CDW) phase exists within the pseudogap regime. This CDW coexists and competes with superconductivity (SC) below the transition temperature T_c, suggesting that these two orders are intimately related. Here we show that the condensation of the superfluid from this unconventional precursor is reflected in deviations from the predictions of BSC theory regarding the recombination rate of quasiparticles. We report a detailed investigation of the quasiparticle (QP) recombination lifetime, τ_{qp}, as a function of temperature and magnetic field in underdoped $HgBa_2CuO_{4+\delta}$ (Hg-1201) and $YBa_2Cu_3O_{6+x}$ (YBCO) single crystals by ultrafast time-resolved reflectivity. We find that $\tau_{qp}(T)$ exhibits a local maximum in a small temperature window near T_c that is prominent in underdoped samples with coexisting charge order and vanishes with application of a small magnetic field. We explain this unusual, non-BCS behavior by positing that T_c marks a transition from phase-fluctuating SC/CDW composite order above to a SC/CDW condensate below. Our results suggest that the superfluid in underdoped cuprates is a condensate of coherently-mixed particle-particle and particle-hole pairs.

First observed as stripe-like order in the "214" cuprates[1], as checkerboard order in vortex cores[2], and subsequently at the surface of Bi and Cl based compounds[3–5], the universality of CDW order in the cuprate phase diagram has been established, through NMR[6] and X-ray scattering[7–12] probes. In $YBa_2Cu_3O_{6+x}$ (YBCO) near hole concentration 1/8 application of large magnetic fields stabilizes long-range CDW order at a temperature that approaches T_c[6,13]. The near-degeneracy of the characteristic temperatures of CDW and SC phases suggests that these two order parameters are related, as opposed to simply coexisting and competing. Several theoretical works have suggested that the same short-range antiferromagnetic fluctuations drive the formation of CDW and SC states[14–18]. Moreover, the temperature dependence of the CDW amplitude in YBCO, as determined from X-ray scattering, can be reproduced by a model of fluctuating, multi-component order, of which CDW and SC states are two projections[17].

The basic premise of BCS theory is that the SC condensate is made up of Cooper pairs, which are bound states of two electrons with opposite momenta and spin[19]. Subsequent to BCS, Kohn and Sherrington[20] showed that a CDW state is likewise a pair condensate, but of electron and holes, whose net momentum determines the wavelength of charge order. Quasiparticles (or broken pairs) are the fundamental excitations of paired condensates

[1]Materials Science Division, Lawrence Berkeley National Laboratory, Berkeley, California 94720, USA. [2]Department of Physics, University of California, Berkeley, California 94720, USA. [3]Department of Physics, University of California, San Diego, California 92093, USA. [4]Department of Physics, Massachusetts Institute of Technology, Cambridge, MA 02139, USA. [5]School of Physics and Astronomy, University of Minnesota, Minneapolis, Minnesota 55455, USA. [6]Institute of Solid State Physics, TU Wien, 1040 Vienna, Austria. [7]Department of Physics and Astronomy, University of British Columbia, Vancouver, Canada. [8]Canadian Inst. Adv. Res., Toronto, ON M5G 178, Canada. [9]Linac Coherent Light Source, SLAC National Accelerator Laboratory, Menlo Park, CA 94025, USA. [10]Department of Physics, North Carolina State University, Raleigh, North Carolina 27695-7518, USA. Correspondence and requests for materials should be addressed to J.P.H. (email: jhinton@ucsd.edu)

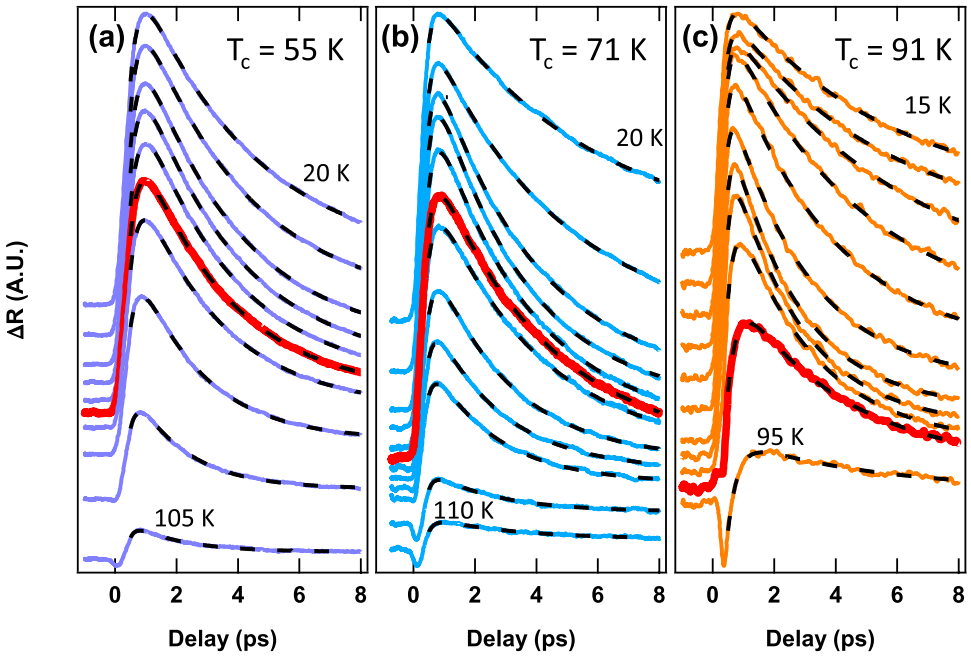

Figure 1. Delay, temperature, and doping dependence of transient reflectivity. Time-dependence of $\Delta R(t, T)/R$ for a range of temperatures that spans T_c is shown for three underdoped samples with $T_c = 55$, 71, and 91 K, in (**a–c**), respectively. Curves are offset for clarity by an amount proportional to the temperature. The quasiparticle recombination time is extracted for each temperature from the exponential fits shown as dashed black lines.

such as the SC and CDW states. It is important for what follows to note that, although quasiparticles in SC and CDW states are fermions, they have properties distinct from the quasiparticles that constitute the normal state. SC quasiparticles are phase-coherent linear superpositions of normal state electrons and holes, while CDW quasiparticles are superpositions of electrons (or holes).

Our experiments probe quasiparticle states in underdoped cuprates through time-resolved measurements of their lifetime against recombination, whereby two quasiparticles of opposite spin re-pair and scatter into the condensate. As we discuss below, this scattering rate is sensitive to the phase-coherence of quasiparticle superposition states. To measure the recombination lifetime, we first generate a nonequilibrium quasiparticle population by photoexcitation with an ultrashort optical pulse. We use a low pump fluence so as to probe the linear regime in which the photogenerated quasiparticle population is small compared to its thermal value near T_c. The rate of return to equilibrium is measured by resolving the photoinduced change in optical reflectivity, $\Delta R(t)$, as a function of time, t, after absorption of the pump pulse. A wealth of experiments[21,22] have demonstrated that the appearance of a ΔR signal reflects the opening of a gap (or gaps) at the Fermi level and that its amplitude is proportional to the nonequilibrium quasiparticle population.

Results

Correlation with CDW order. In Fig. 1 we show $\Delta R(t)/R$ at several temperatures for underdoped samples of Hg-1201 with $T_c = 55$, 71, and 91 K. At high temperature we observe a short-lived negative component of $\Delta R(t)$ that is associated with the pseudogap (PG)[23]. With decreasing T a larger amplitude positive component with a much longer lifetime appears and quickly dominates the signal. In cuprates with near-optimal doping this positive, long-lived component appears close to T_c[24] and was therefore associated with the onset of superconductivity. However, this association breaks down in underdoped samples in which the positive component is already large at T_c (data at T_c are highlighted in red).

In Fig. 2a–f we plot the maximum value of $\Delta R/R(t)$ (which occurs at ≈1 ps after photoexcitation) as a function of T in underdoped Hg-1201 samples with T_c's ranging from 55 to 91 K. The temperature (T_{onset}) at which the positive component of ΔR appears is indicated by a blue down arrow in each panel. Note that ΔR continues to increase continuously with further decrease of T, without a clear feature at the critical temperature for superconductivity (indicated by red arrows). Both T_{onset} and T_c are plotted as a function of hole concentration, p, in Fig. 2g. The onset temperatures of positive ΔR outline a dome that peaks on the underdoped side of the phase diagram and extends to temperatures 130 K above T_c.

Based on a correlations with other probes, we believe that the appearance of the slow, positive component of ΔR at the temperatures $T_{onset}(p)$ shown in Fig. 2g corresponds to the onset of local CDW order. There is a clear correspondence between the dome of T_{onset} as determined by $\Delta R(T)$ in Hg-1201 and the region of the phase diagram where a CDW is detected in YBCO[25,26]. Although the phase space region of CDW in Hg-1201 is yet to be mapped in as much detail as in YBCO, a CDW has been detected in Hg-1201 samples with $T_c = 71$ K[12] at a

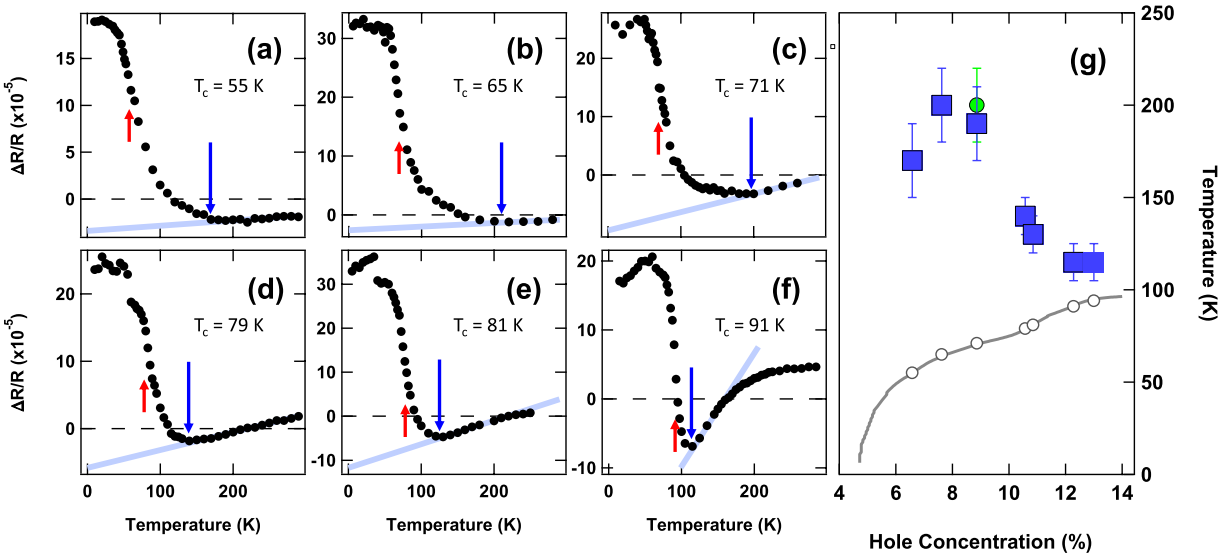

Figure 2. Doping dependence of onset temperature. (**a**–**f**) The temperature dependence of $\Delta R(t = 1\,\text{ps})/R$ is plotted for a series of doping levels. Values of T_{onset} as determined from the inflection points of the curves are indicated by the vertical blue arrows, and T_c is indicated by red arrows. (**g**) T_{onset} as function of hole concentration, p, as obtained from the inflection points in (**a**–**f**) are plotted as blue squares in a $T-p$ phase diagram for the Hg-1201 system. Also shown is the onset temperature of charge order observed by X-ray scattering[12] (green circle) and the critical temperatures for superconductivity (open circles).

temperature (indicated by the green circle in Fig. 2g) coincident with T_{onset}. Another correlation linking ΔR to the CDW in underdoped cuprates is that the positive component of ΔR in YBCO Ortho-VIII (to be discussed further below) has the same temperature dependence as a zero wavevector vibrational mode that arises from CDW-induced zone-folding[27].

Recombination lifetime. We turn now to measurements of the T dependence of the recombination lifetime of quasiparticles for $T < T_{onset}$. The decay curves in Fig. 1 were fit using a function of the form, $\Delta R(t) \propto Ae^{-t/\tau_{qp}} - Be^{-t/\tau_r} + C$, where the first term describes QP recombination, the second term accounts for finite risetime and the presence of a negative PG component, and the constant offset C captures a long-lived contribution that we attribute to local heating by the pump pulse (see Supplement for details on the fitting procedure). Figure 3a displays the evolution of $\tau_{qp}(T)$ with hole concentration in the Hg-1201 system. At each hole concentration we observe structure in the T-dependence of the quasiparticle recombination time at T_c. In underdoped samples there is a peak in $\tau_{qp}(T)$ at T_c that is most prominent in the $T_c = 71$ K sample and decreases in amplitude at lower and slightly higher hole concentration in a manner that appears to be correlated with the strength of the CDW.

Figure 3b,c compare $\Delta R(t, T)$ in Hg-1201 ($T_c = 71$ K) and YBCO Ortho-VIII ($T_c = 67$ K), illustrating that generality of the phenomena described above. Figure 3b,c show the temperature dependence of the amplitude $\Delta R_{qp} \equiv A$ and τ_{qp} respectively for the two underdoped samples. In both we observe the onset of positive $\Delta R(T)$ well above T_c and a smooth variation through the SC transition. As shown in Fig. 3c, peak in $\tau_{qp}(T)$ centered on T_c is strikingly similar in the two representative samples.

The T-dependence of the quasiparticle lifetime in the sample of Hg-1201 at near-optimal doping (topmost data set of Fig. 3a) is qualitatively different from what is seen in underdoped samples. In the near-optimal sample τ_{qp} grows monotonically as $T \rightarrow T_c$, suggesting a tendency to diverge as $\Delta R_{qp}(T)$ goes to zero, while in underdoped samples the peak in τ_{qp} at T_c is a small feature on a smooth background. The behavior of τ_{qp} in near-optimal Hg-1201, which is observed in other optimally doped cuprates as well[24,28], can be understood within the mean-field theory of superconductivity. The theoretical description of $\tau_{qp}(T)$ in the context of BCS began in the 1960's and its subsequent history is reviewed in ref. 29. In the mean-field picture, the relaxation of a nonequilibrium quasiparticle population is described by a pair of coupled equations: a Landau-Khalatnikov equation for the energy gap and a Boltzmann-like equation that governs the quasiparticle distribution[29]. According this analysis, $\tau_{qp}(T) \propto \tau T/\Delta(T)$ (where τ is the electron inelastic scattering time) and diverges as the superconducting gap $\Delta(T)$ vanishes as T approaches T_c from below. In more recent work on cuprate superconductors, effects associated with the phonon bottleneck[28,30–32] are included, which leads to replacing τ by the lifetime of phonons with energy greater than 2Δ.

Phase coherence and recombination. The behavior of $\tau_{qp}(T)$ in underdoped samples is at odds with the mean-field picture described above. Two observations–continuous variation of ΔR_{qp} for $T < T_{onset}$ and the smoothly varying background in $\tau_{qp}(T)$ that underlies the small peak–suggest that a quasiparticle gap has opened

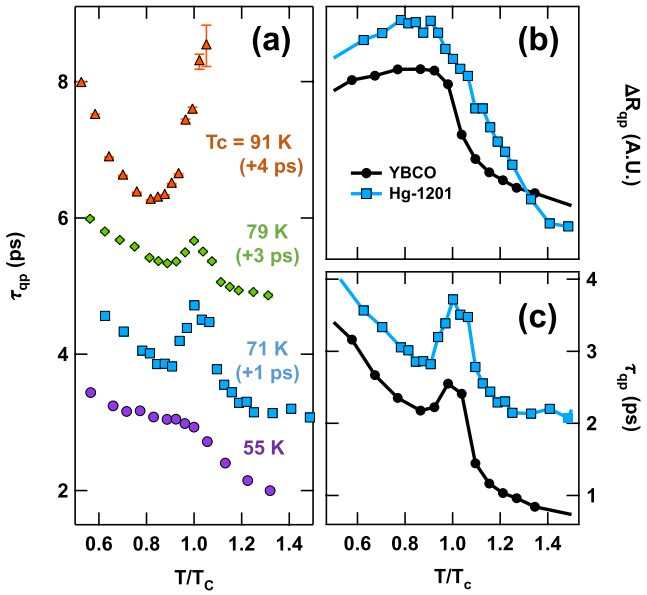

Figure 3. Quasiparticle recombination lifetime. (**a**) Temperature dependence of τ_{qp} for a series of underdoped Hg-1201 samples. Curves are offset for clarity, as indicated in the figure. (**b**) Temperature dependence of the positive component of the transient reflectivity, ΔR_{QP} and (**c**) the quasiparticle lifetime, τ_{qp}, for YBCO Ortho VIII with $T_c = 67$ K (black circles) and Hg-1201 with $T_c = 71$ K (blue squares). The temperature axis is normalized to T_c.

well above T_c. Given a pre-existing gap, it is very difficult to explain the modulation of the quasiparticle lifetime near T_c. In view of the difficulties with the mean-field picture, we are led to consider the onset of phase coherence at T_c, rather than gap-opening, as the origin of the structure in $\tau_{qp}(T)$.

Coherence effects have been observed previously elastic QP scattering, as detected by QP interference in scanning tunneling microscopy experiments[2,33,34]. However, the implications of coherence for a process in which two quasiparticles scatter into the condensate have not previously been considered in the context of the cuprates. In a phase-incoherent state the recombination rate is proportional to the square modulus of the interaction matrix element between electrons and holes. In a phase-coherent paired state, recombination is more complex because, as mentioned previously, QPs are linear superpositions of electrons and holes. As a result, the matrix element for recombination reflects multiple channels that can interfere constructively or destructively, depending on the nature of the pairing state and QP interactions[19].

The rate of QP recombination in a paired condensate is the product of the normal state rate and a "coherence factor" (F) that is a function of the Bogoliubov coefficients u and v. For the case of time-reversal invariant QP interactions the coherence factors for SC and CDW condensates are given by

$$F_{SC} = (vu' - uv')^2 = \frac{1}{2}\left(1 + \frac{\Delta\Delta'}{EE'}\right) \quad (1)$$

$$F_{CDW} = \frac{1}{2}\left(1 - \frac{\Phi\Phi'}{EE'}\right) \quad (2)$$

where Δ and Δ' are the amplitudes of the SC gap at the two QP momenta, Φ and Φ' are the analogous CDW gaps, and E and E' are the QP energies[35]. In the limit that E and E' approach the gap energy, these factors reduce to $F_{SC} = 1$ and $F_{CDW} = 0$, while in the normal state $F = 1/2$. We note that the result $F_{CDW} = 0$ is related to the π phase shift between occupied and unoccupied states, which has recently been observed in CDW states in Bi2212[36].

The simplest scenario, in which a phase-fluctuating superconductor becomes fully phase coherent at T_c, is inconsistent with a peak in $\tau_{qp}(T)$ (or local minimum in recombination rate). Instead, SC coherence yields a doubling of the recombination rate, corresponding to the factor of two jump in F from 1/2 to 1 upon crossing from a normal to SC state. However, we have found that a model that takes into account the dual presence of fluctuating CDW and SC order leads to a singular feature in $\tau_{qp}(T)$ that agrees well with experiment.

Fluctuation of composite SC-CDW order. To formulate this model quantitatively, we derived the recombination coherence factor for a state with coexisting SC and CDW order. The composite SC/CDW condensate is made of particle-hole quadruplets, pairing electrons at $\pm k$ and holes at $\pm(k+Q)$ separated by the CDW wavevector Q. The structure of the quasiparticle eigenstates of the composite SC/CDW condensate is shown schematically in Fig. 4a. Based on these eigenstates, we determined the dependence of the mixed state coherence factors on

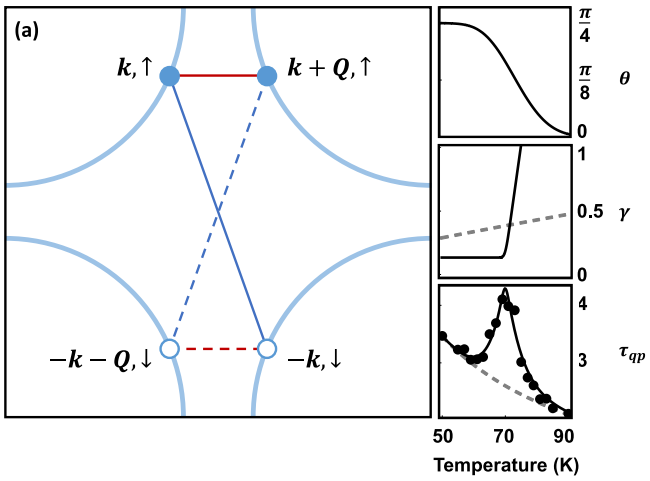

Figure 4. Mixed-state coherence factors. (**a**) Momentum space diagram of the electron eigenstates that determine the rate of quasiparticle recombination. The region defined by the square is the first Brillouin zone of a cuprate superconductor - inside are the four "Fermi arcs" shown as blue curves. The pairing of electrons and holes at k and $k+Q$ drives CDW formation, whereas electron pairing at k, $-k$ states (blue lines) is responsible for superconductivity. Quasiparticles are excited states of paired condensates formed from a superposition of two normal phase electron eigenstates. CDW quasiparticles, represented by the red lines, are superpositions of electrons at k and $k+Q$, whereas SC quasiparticles, represented by blue lines, are superpositions of electrons and holes. In the mixed SC-CDW condensate that forms in underdoped cuprate superconductors, quasiparticles become superpositions of four, rather than just two electron eigenstates. The rate at which such quasiparticles scatter back into the condensate depends sensitively on the mixing angle of SC and CDW components, as well as on the condensate phase-correlation time. The temperature dependent mixing angle, $\theta(T)$ (shown in (**b**)), phase fluctuation rate, $\tau_c^{-1}(T)$ (solid line in (**c**)), and reciprocal of the normal state lifetime, $\tau_0^{-1}(T)$ (gray dashed line in (**c**)) produce the fit to the quasiparticle lifetime in the Hg-1201 ($T_c = 71$ K) sample displayed in (**d**).

the quasiparticle energy (see Methods). As time and angle-resolved photoemission measurements observe rapid thermalization of quasiparticles to gap edge after photo-excitation[37,38], we focus on the coherence factor in the limit that $E, E' \to \Delta, \Delta'$ which simplifies the expression for F considerably. In this limit, the QP recombination coherence factor becomes,

$$F = \frac{1}{2}\left(1 + \cos\phi_\Delta \frac{\Delta^2}{\Delta^2 + \Phi^2} - \cos\phi_\Phi \frac{\Phi^2}{\Delta^2 + \Phi^2}\right) \tag{3}$$

where ϕ_Δ and ϕ_Φ are the relative phases of the QP pair undergoing recombination. In the case of d-wave pairing, these phases will be 0 or π, depending on which k points the QPs occupy. STM QP interference demonstrates that the strongest scattering channels are between states with the same sign of gap amplitude[34], so we restrict our attention to these recombination processes.

In the presence of phase fluctuations, the $\cos\phi$ factors are replaced by their ensemble average $\langle\cos\phi\rangle = e^{-\tau_0/\tau_c}$, where τ_c is the phase-correlation time and τ_0 is the QP lifetime in the fully incoherent regime. The coherence factor obtained by this substitution would apply to systems with coexisting, but independent, CDW and SC order. However, in the light of evidence that these orders are strongly coupled in underdoped cuprates, we consider a description in terms of a multi-component order parameter[17] whose amplitude $\sqrt{\Phi^2 + \Delta^2}$ is constant and whose fluctuations are described by a single phase ϕ. With these assumptions the coherence factor can be written,

$$\langle F\rangle = \frac{1}{2}(1 - e^{-\tau_0/\tau_c}\cos 2\theta), \tag{4}$$

where $\tan^2\theta \equiv \Phi^2/\Delta^2$.

Figure 4d shows a fit to $\tau_{qp}(T)$ for the Hg-1201 $T_c = 71$ K sample using Eq. 4. Figure 4b,c show the temperature dependence of the three parameters from which the fits were generated. The mixing angle $\theta(T)$ is plotted in Fig. 4b. The reciprocal of the coherence time, τ_c^{-1}, and reciprocal of the incoherent recombination time, $\tau_0^{-1}(T)$, are plotted as solid and dashed lines, respectively in Fig. 4c. The T-dependence of τ_0 is determined by a polynomial fit to $\tau_{qp}(T)$ that ignores the peak at T_c. The quasiparticle decoherence rate τ_c^{-1} is constrained to be constant below T_c and to vary $\propto(T - T_c)$ above the transition, as suggested by angle-resolved photoemission spectra[39]. The slope of τ_c^{-1} vs. $T - T_c$ extracted from our fit ($\approx$0.15 THz/K) is consistent with estimates of coherence times obtained from optical conductivity[40]. The peak in $\tau_{qp}(T)$ shown in Fig. 4d arises from the interplay between the mixing angle $\theta(T)$ and the onset of quasiparticle coherence. Starting at temperatures well above T_c, the order parameter is CDW-like with a short coherence time. As the temperature is lowered towards T_c and the CDW

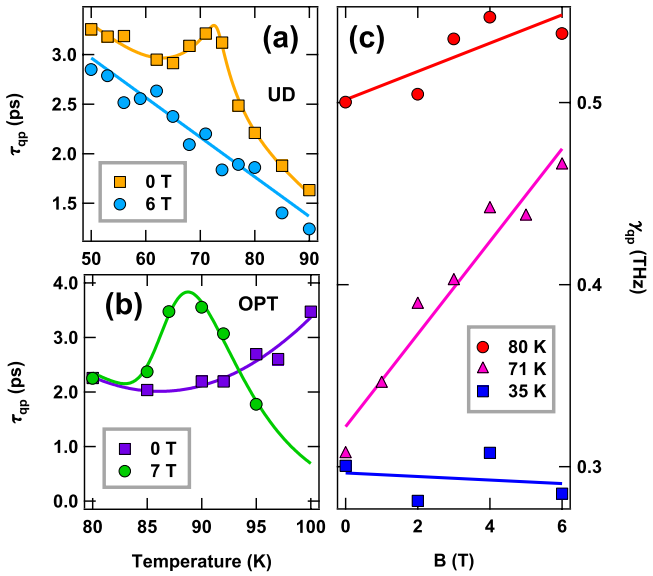

Figure 5. Magnetic field dependence. (**a**) Temperature dependence of the recombination time τ_{qp} in zero field and 6 Tesla applied normal to the surface of Hg-1201 ($T_c = 71$ K). (**b**) Temperature dependence of τ_{qp} at 0 and 7 Tesla in Hg-1201 ($T_c = 94$) K. (**c**) The quasiparticle recombination rate, γ_{qp}, at 35 K, at $T_c = 71$ K, and at 80 K, plotted vs H for the underdoped Hg-1201 sample with $T_c = 71$ K.

becomes more coherent, $\langle F \rangle$ dips below its normal state value of 1/2 and the QP lifetime is enhanced. However, as the order parameter crosses over from CDW to SC-like near T_c, $\langle F \rangle$ increases, giving rise to a peak τ_{qp}.

Magnetic field effect. To further examine the relationship between phase coherence and quasiparticle recombination, we investigated the effect of magnetic field, B, on $\tau_{qp}(T)$. An overview of $\tau_{qp}(B,T)$ in fields applied perpendicular to the Cu-O planes is shown in Fig. 5. Figure 5a compares the quasiparticle lifetime in zero field and 6 Tesla for a sample of Hg-1201 with $T_c = 71$ K. The peak in $\tau_{qp}(T)$ is entirely washed out by the field and replaced by a smooth background that is described by the model parameter $\tau_0(T)$ discussed previously. In Fig. 5c, the change in recombination rate caused by the field, $\Delta\gamma_{qp}(B) \equiv \tau_{qp}^{-1}(B) - \tau_{qp}^{-1}(0)$, is plotted vs. B at three temperatures: well below, above, and at T_c. It is clear that strong dependence of τ_{qp} on B is observed only near T_c. The field dependence of the quasiparticle lifetime is qualitatively different in the near optimal Hg-1201 sample (shown in Fig. 5b), where we find that the maximum τ_{qp} shifts to lower T but is not reduced, consistent with what is expected for a mean-field gap opening transition.

The B dependence of τ_{qp} can be understood to be a consequence of dephasing in the vortex liquid induced by the field. Assuming a total dephasing rate, $\tau_c^{-1} + \Gamma(B)$, where $\Gamma(B)$ is the dephasing rate associated with vortex diffusion, yields

$$\Delta\gamma_{qp}(B) = [\tau_{qp}^{-1}(T_c) - \tau_0^{-1}(T_c)/2]\{1 - \exp[-\Gamma(B)\tau_0]\}. \quad (5)$$

The dashed line in Fig. 5c is a fit to this functional form, with $\Gamma(B) = (0.08\,\mathrm{THz/T})B$. This result can be compared with the theory of phase fluctuations in the vortex liquid[41], where it is shown that $\Gamma(B) \simeq (\xi/l_B)^2 k_B T_c/\hbar$, where ξ and l_B are the coherence and magnetic length, respectively. Equating this estimate with the measured $\Gamma(B)$ yields a reasonable value for the coherence length of 2.4 nm, strongly suggesting that B-induced dephasing accounts for wipeout of the τ_{qp} peak.

Summary. To summarize, we have described measurements and analysis of the photoinduced transient reflectivity, $\Delta R(t,T)$ in representative YBCO and Hg-1201 samples of underdoped cuprates. The onset of ΔR with decreasing temperature is correlated with the appearance of the incommensurate CDW detected previously by NMR, STM, and X-ray scattering measurements. This correlation leads us to conclude that, although the density of states depression known as the pseudogap is formed at a higher temperature, the CDW either enhances it, or leads to a new gap of different origin. A correlation between CDW and gap formation is suggested as well by recent ARPES measurements[42,43]. We focused attention on two aspects of $\Delta R(t)$ as T was lowered through T_c. In underdoped samples, ΔR increases continuously through T_c, suggesting a smooth variation of the gap at the Fermi surface hot spots (or Fermi-arc tips). Second, while the gap varies continuously, the quasiparticle recombination time exhibits a narrow local maximum at T_c. We proposed that this peak in τ_{qp} indicates a crossover from fluctuating CDW to SC/CDW order, occurring as the condensate coherence time slides through the time window set by the background recombination time ~2–3 ps. The link between condensate coherence and the peak in $\tau_{qp}(T)$ was further supported by the observation that magnetic field causes the peak to disappear into the

background. Our results show that quasiparticle recombination provides a new method for probing the onset of coherence in systems characterized by a fluctuating multi-component order parameter.

Materials and Methods

Hg-1201 synthesis and preparation. We examined a series of high quality single crystals of Hg-1201 ranging from deeply underdoped to optimal doping with T_c's of 55 K, 65 K, 71 K, 79 K, 81 K, 91 K, and 94 K. These samples were grown by the self-flux method[44] and annealed to achieve different oxygen concentrations[45], with T_c determined within ~1 K by magnetic susceptibility measurements. Hole concentration was determined using methods described in ref. 46. Samples were polished under nitrogen flow using 0.3 μm grit films to prevent surface oxidation.

Ultrafast Measurements. The measurements reported herein were performed using 100 fs pulses from a mode-locked Ti:Sapphire laser at 800 nm center wavelength and $\simeq 1\,\mu J/cm^2$ fluence. Pump pulses induced a small ($\sim 10^{-4}$) fractional change in reflectivity that was monitored by time-delayed probe pulses. At the low laser fluence used in this study, samples are weakly perturbed by the pump pulse, in the sense that the density of photogenerated quasiparticles is much less than the thermal equilibrium value. In this regime the decay rate is a measure of the quasiparticle recombination rate in thermal equilibrium. Measurements in zero magnetic field at Berkeley were performed under vacuum in an Oxford continuous-flow liquid He cryostat. Magneto-optic measurements at Berkeley were performed in a 6T Oxford Spectramag cryostat, and those at MIT in a 7T Janis cryostat.

Calculation of mixed-state coherence factors. The mean-field Hamiltonian is given by $\mathcal{H}_{SC+CDW} = \Sigma_{\mathbf{k}} A_{\mathbf{k}}^{\dagger} M A_{\mathbf{k}}$[47], with

$$A_{\mathbf{k}}^{\dagger} = \left(a_{\mathbf{k}\uparrow}^{\dagger} \;\; a_{(\mathbf{k}\pm Q)\uparrow}^{\dagger} \;\; a_{-\mathbf{k}\downarrow} \;\; a_{-(\mathbf{k}\pm Q)\downarrow}\right) \tag{6}$$

$$M = \begin{pmatrix} \xi_{\mathbf{k}} & \Phi & \Delta & 0 \\ \Phi^* & \xi_{\mathbf{k}\pm Q} & 0 & \Delta \\ \Delta^* & 0 & -\xi_{-k} & -\Phi \\ 0 & \Delta^* & -\Phi^* & -\xi_{-(\mathbf{k}\pm Q)} \end{pmatrix} \tag{7}$$

Diagonalizing the CDW and SC subsystems via successive Bogoliubov transformations yields energy eigenvalues $E_{\mathbf{k}}^2 = \pm(\xi_{\mathbf{k}}^2 + \Delta^2 + \Phi^2)$. The eigenvectors give the composite QP operators $\Gamma_{\mathbf{k}}^{\dagger} = A_{\mathbf{k}}^{\dagger} B$, where

$$\Gamma_{\mathbf{k}}^{\dagger} = (\gamma_{\mathbf{k}\alpha 0}^{\dagger} \;\; \gamma_{\mathbf{k}\beta 1}^{\dagger} \;\; \gamma_{\mathbf{k}\beta 0}^{\dagger} \;\; \gamma_{\mathbf{k}\alpha 1}^{\dagger}) \tag{8}$$

$$B = \begin{pmatrix} su & tu & sv & tv \\ -t^*u & su & t^*v & -sv \\ -sv^* & -tv^* & su & tu \\ -t^*v^* & sv^* & -t^*u & su \end{pmatrix} \tag{9}$$

$$|s_{\mathbf{k}}|^2 = 1 - |t_{\mathbf{k}}|^2 = \frac{1}{2}\left(1 + \frac{\xi_{\mathbf{k}}}{\sqrt{\xi_{\mathbf{k}}^2 + \Phi^2}}\right) \tag{10}$$

$$|u_{\mathbf{k}}|^2 = 1 - |v_{\mathbf{k}}|^2 = \frac{1}{2}\left(1 + \frac{\sqrt{\xi_{\mathbf{k}}^2 + \Phi^2}}{\sqrt{\xi_{\mathbf{k}}^2 + \Phi^2 + \Delta^2}}\right) \tag{11}$$

In the above, u and s are assumed to be real, and the phases of v and t are determined by the phases of Δ and Φ, respectively. We calculate the coherence factors following ref. 48, starting with a quasiparticle interaction of the form $\mathcal{H}_{int} = \Sigma_{\mathbf{k}} I_{\mathbf{k}'\sigma'\mathbf{k}\sigma} a_{\mathbf{k}'\sigma'}^{\dagger} a_{\mathbf{k}\sigma}$. We assume that the interaction is spin-independent. The four four electronic transitions that involve the same QP operators,

$$a_{\mathbf{k}'\uparrow}^{\dagger} a_{\mathbf{k}\uparrow} + a_{(\mathbf{k}'\pm\mathbf{Q})\uparrow}^{\dagger} a_{(\mathbf{k}\pm\mathbf{Q})\uparrow} \tag{12}$$

$$+ a_{-\mathbf{k}\downarrow}^{\dagger} a_{-\mathbf{k}'\downarrow} + a_{(-\mathbf{k}\pm\mathbf{Q}\uparrow)}^{\dagger} a_{-(\mathbf{k}'\pm\mathbf{Q})\uparrow} \tag{13}$$

must be summed coherently before calculating the squared modulus of the matrix element that determines the quasiparticle scattering rate. Expressing the four bilinear operators in terms of the quasiparticle (γ) operators yields,

$$f_1 \gamma_{\mathbf{k}\alpha 0} \gamma_{\mathbf{k}'\beta 0} + f_1^* \gamma_{\mathbf{k}\alpha 1} \gamma_{\mathbf{k}'\beta 1} \tag{14}$$

$$+f_2\,\gamma_{\mathbf{k}\alpha 0}\gamma_{\mathbf{k}'\beta 1} + f_2^{*}\,\gamma_{\mathbf{k}\alpha 1}\gamma_{\mathbf{k}'\beta 0} \tag{15}$$

where,

$$f_1 = usv's' + utv't'^{*} + vsu's' + vtu't'^{*} \tag{16}$$

$$f_2 = ut^{*}u's' - usu't'^{*} + vt^{*}v's' - v^{*}sv't'^{*} \tag{17}$$

and $u' \equiv u_{\mathbf{k}'}$. Summing over recombination channels and then squaring yields a coherence factor for quasiparticle recombination given by $F = |f_1|^2 + |f_2|^2$.

References

1. Tranquada, J. M., Sternlieb, B. J., Axe, J. D., Nakamura, Y. & Uchida, S. Evidence for stripe correlations of spins and holes in copper oxide superconductors. *Nature* **375,** 561–563 (1995).
2. Hoffman, J. *et al.* A four unit cell periodic pattern of quasi-particle states surrounding vortex cores in $Bi_2Sr_2CaCu_2O_{8+\delta}$. *Science* **295,** 466–469 (2002).
3. Howald, C., Eisaki, H., Kaneko, N. & Kapitulnik, A. Coexistence of periodic modulation of quasiparticle states and superconductivity in $Bi_2Sr_2CaCu_2O_{8+\delta}$. *Proc. Natl Acad. Sci. USA* **100,** 9705–9709 (2003).
4. Vershinin, M. *et al.* Local ordering in the pseudogap state of the high-T_c superconductor $Bi_2Sr_2CaCu_2O_{8+\delta}$. *Science* **303,** 1995–1998 (2004).
5. Wise, W. D. *et al.* Charge-density-wave origin of cuprate checkerboard visualized by scanning tunnelling microscopy. *Nat. Phys.* **4,** 696–699 (2008).
6. Wu, T. *et al.* Magnetic-field-induced charge-stripe order in the high-temperature superconductor $Yba_2Cu_3O_y$. *Nature* **477,** 191–194 (2011).
7. Ghiringhelli, G. *et al.* Long-range incommensurate charge fluctuations in (Y, Nd) $Ba_2Cu_3O_{6+x}$. *Science* **337,** 821–825 (2012).
8. Chang, J. *et al.* Direct observation of competition between superconductivity and charge density wave order in $Yba_2Cu_3O_{6.67}$. *Nat. Phys.* **8,** 871–876 (2012).
9. Le Tacon, M. *et al.* Inelastic X-ray scattering in $Yba_2Cu_3O_{6.6}$ reveals giant phonon anomalies and elastic central peak due to charge-density-wave formation. *Nat. Phys.* **10,** 52–58 (2014).
10. Comin, R. *et al.* Charge order driven by Fermi-arc instability in $Bi_2Sr_{2-x}La_xCuO_{6+\delta}$. *Science* **343,** 390–392 (2014).
11. da Silva Neto, E. H. *et al.* Ubiquitous interplay between charge ordering and high-temperature superconductivity in cuprates. *Science* **343,** 393–396 (2014).
12. Tabis, W. *et al.* Charge order and its connection with Fermi-liquid charge transport in a pristine high-T_c cuprate. *Nat. Commun.* **5,** 5875 (2014).
13. LeBoeuf, D. *et al.* Thermodynamic phase diagram of static charge order in underdoped $Yba_2Cu_3O_y$. *Nat. Phys.* **9,** 79–83 (2013).
14. Efetov, K. B., Meier, H. & Pépin, C. Pseudogap state near a quantum critical point. *Nat. Phys.* **9,** 442–446 (2013).
15. Sachdev, S. & La Placa, R. Bond order in two-dimensional metals with antiferromagnetic exchange interactions. *Phys. Rev. Lett.* **111,** 027202 (2013).
16. Davis, J. C. & Lee, D. H. Concepts relating magnetic interactions, intertwined electronic orders, and strongly correlated superconductivity. *Proc. Natl Acad. Sci. USA* **110,** 17623–17630 (2013).
17. Hayward, L. E., Hawthorn, D. G., Melko, R. G. & Sachdev, S. Angular fluctuations of a multicomponent order describe the pseudogap of $Yba_2Cu_3O_{6+\delta}$. *Science* **343,** 1336–1339 (2014).
18. Wang, Y. & Chubukov, A. A Charge-density-wave order with momentum (2*Q*, 0) and (0, 2*Q*) within the spin-fermion model: Continuous and discrete symmetry breaking, preemptive composite order, and relation to pseudogap in hole-doped cuprates. *Phys. Rev. B* **90,** 035149 (2014).
19. Schrieffer, J. R. *Theory of Superconductivity* (W.A. Benjamin, New York 1964).
20. Kohn, W. & Sherrington, D. Two kinds of bosons and bose condensates. *Rev. Mod. Phys.* **42,** 1 (1970).
21. Averitt, R. A. & Talor, A. J. Ultrafast optical and far-infrared quasiparticle dynamics in correlated electron materials. *J. Phys. Condens. Matter* **14,** R1357 (2002).
22. Giannetti, C., Capone, M., Fausti, D., Fabrizio, M., Parmigiani, F. & Mihailovic, D. Ultrafast optical spectroscopy of strongly correlated materials and high-temperature superconductors: a non-equilibrium approach. *arXiv:1601.07204* (2016).
23. Demsar, J. *et al.* Superconducting gap Δ_c, the pseudogap Δ_p, and pair fluctuations above T_c in overdoped $Y_{1-x}Ca_xBa_2Cu_3O_{7-\delta}$ from femtosecond time-domain spectroscopy. *Phys. Rev. Lett.* **82,** 4918 (1999).
24. Han, S. G., Vardeny, Z. V., Wong, K. S., Symko, O. G. & Koren, G. Femtosecond optical detection of quasiparticle dynamics in high-T_c $Yba_2Cu_3O_7$ superconducting thin films. *Phys. Rev. Lett.* **65,** 2708–2711 (1990).
25. Hücker, M. *et al.* Competing charge, spin and superconducting orders in $Yba_2Cu_3O_y$. *Phys. Rev. B* **90,** 054514 (2014).
26. Blanco-Canosa, S., *et al.* Resonant x-ray scattering study of charge-density wave correlations in $Yba_2Cu_3O_{6+x}$. *Phys. Rev. B* **90,** 054513 (2014).
27. Hinton, J. P. *et al.* New collective mode in $Yba_2Cu_3O_{6+x}$ observed by time-domain reflectometry. *Phys. Rev. B* **88,** 060508(R) (2013).
28. Kabanov, V. V., Demsar, J., Podobnik, B. & Mihailovic, D. Quasiparticle relaxation dynamics in superconductors with different gap structures: Theory and experiments on $Yba_2Cu_3O_{7-\delta}$. *Phys. Rev. B* **59,** 1497–1506 (1999).
29. Schuller, I. K. & Gray, K. E. Time-dependent Ginzburg–Landau: from single particle to collective behavior. *J. Superconductivity and Novel Magnetism* **19,** 401–407 (2006).
30. Rothwarf, A. & Taylor, B. N. Measurement of recombination lifetimes in superconductors. *Phys. Rev. Lett.* **19,** 27 (1967).
31. Gedik, N. *et al.* Single-quasiparticle stability and quasiparticle-pair decay in $Yba_2Cu_3O_{6.5}$. *Phys. Rev. B* **70,** 014504 (2004).
32. Kabanov, V. V., Demsar, J. & Mihailovic, D. Kinetics of a superconductor excited with a femtosecond optical pulse. *Phys. Rev. Lett.* **95,** 147002 (2005).
33. Hanaguri, T. *et al.* Coherence factors in a high-T_c cuprate probed by quasi-particle scattering off vortices. *Science* **323,** 923–926 (2009).
34. Lee, J. *et al.* Spectroscopic fingerprint of phase-incoherent superconductivity in the underdoped $Bi_2Sr_2CaCu_2O_{8+\delta}$. *Science* **325,** 1099–1103 (2009).
35. Grüner, G. *Density Waves in Solids* (Addison-Wesley, Reading, MA, 1994).
36. Hamidian, M. *et al.* Atomic-scale electronic structure of the cuprate d-symmetry form factor density wave state. *Nat. Phys.* **12,** 150–156 (2016).
37. Smallwood, C. L. *et al.* Tracking Cooper pairs in a cuprate superconductor by ultrafast angle-resolved photoemission. *Science* **336,** 1137–1139 (2012).

38. Smallwood, C. L. *et al.* Influence of optically quenched superconductivity on quasiparticle relaxation rates in $Bi_2Sr_2CaCu_2O_{8+\delta}$. *Phys. Rev. B* **92,** 161102(R) (2015).
39. Norman, M. R., Randeria, M., Ding, H. & Campuzano, J. C. Phenomenology of the low-energy spectral function in high-T_c superconductors. *Phys. Rev. B* **57,** R11093 (1998).
40. Corson, J., Mallozzi, R., Orenstein, J., Eckstein, J. N. & Bozovic, I. Vanishing of phase coherence in underdoped $Bi_2Sr_2CaCu_2O_{8+\delta}$. *Nature* **398,** 221–223 (1999).
41. Halperin, B. I. & Nelson, D. R. Resistive transition in superconducting films. *J. Low Temp. Phys.* **36,** 599–616 (1979).
42. Hashimoto, M. *et al.* Particle-hole symmetry breaking in the pseudogap state of Bi2201. *Nat. Phys.* **6,** 414–418 (2010).
43. He, R. H. *et al.* From a single-band metal to a high-temperature superconductor via two thermal phase transitions. *Science* **331,** 1579–1583 (2011).
44. Zhao, X. *et al.* Crystal growth and characterization of the model high-temperature superconductor $HgBa_2CuO_{4+\delta}$. *Advanced Materials* **18,** 3243–3247 (2006).
45. Barišić, N. *et al.* Demonstrating the model nature of the high-temperature superconductor $HgBa_2CuO_{4+\delta}$. *Phys. Rev. B* **78,** 054518 (2008).
46. Yamamoto, A., Hu, W.-Z. & Tajima, S. Thermoelectric power and resistivity of $HgBa_2CuO_{4+\delta}$ over a wide doping range, *Phys. Rev. B* **63,** 024504 (2000).
47. Levin, K., Mills, D. L. & Cunningham, S. L. Incompatibility of BCS pairing and the Peierls distortion in one-dimensional systems. I. Mean-field theory. *Phys. Rev. B* **10,** 3821 (1974).
48. Tinkham, M. *Introduction to Superconductivity 2nd edition* (Dover Publications, Mineola, New York 1996).

Acknowledgements

We acknowledge J. C. Davis for enlightening discussions, as well as Lina Ji for assistance with crystal growth. Synthesis and characterization of Hg-1201 samples performed at the University of Minnesota was supported by the Department of Energy, Office of Basic Energy Sciences, under Award No. DE-SC0006858. N.B. acknowledges the support of FWF project P2798. Optical measurements and modeling performed at Lawrence Berkeley National Lab was supported by the Director, Office of Science, Office of Basic Energy Sciences, Materials Sciences and Engineering Division, of the U.S. Department of Energy under Contract No. DE-AC02-05CH11231.

Author Contributions

J.H. and J.O. planned the experiment and analyzed the results. J.H., E.T., J.K., Z.A. and F.M. performed the optical experiments in J.O. and N.G.'s laboratories. J.H. and A.K. performed coherence factor calculations. Hg-1201 samples were grown by M.C., M.V., C.D. and N.B. in M.G.'s laboratory. D.B., W.H. and R.L. grew the YBCO samples. J.H. and J.O. wrote the manuscript, with contributions from M.G., N.G. and A.L. All authors reviewed the manuscript.

Additional Information

Supplementary information accompanies this paper at http://www.nature.com/srep

Competing financial interests: The authors declare no competing financial interests.

How to cite this article: Hinton, J. P. *et al.* The rate of quasiparticle recombination probes the onset of coherence in cuprate superconductors. *Sci. Rep.* **6**, 23610; doi: 10.1038/srep23610 (2016).

This work is licensed under a Creative Commons Attribution 4.0 International License. The images or other third party material in this article are included in the article's Creative Commons license, unless indicated otherwise in the credit line; if the material is not included under the Creative Commons license, users will need to obtain permission from the license holder to reproduce the material. To view a copy of this license, visit http://creativecommons.org/licenses/by/4.0/